Chromatically-corrected, high-efficiency, multi-colour, multi-plane 3D imaging

Chromatically-corrected, high-efficiency, multi-colour, multi-plane 3D imaging

Yan Feng,[1,2] Paul A Dalgarno,[2] David Lee,[3] Yi Yang,[2] Robert R Thomson,[4] and Alan H Greenaway[2,*]

[1]*Department of Precision Machinery and Precision Instrumentation, University of Science and Technology of China, Hefei, Anhui, 230027, China*
[2]*Institute of Biological Chemistry, Biophysics and Bioengineering / SUPA, School of Engineering and Physical Science, Heriot-Watt University, Edinburgh, EH14 4AS, UK*
[3]*UK Astronomy Technology Centre, Blackford Hill, Edinburgh, EH9 3HJ, UK*
[4]*Institute of Photonics and Quantum Sciences / SUPA, School of Engineering and Physical Science, Heriot-Watt University, Edinburgh, EH14 4AS, UK*
[*] *a.h.greenaway@hw.ac.uk*

Abstract: It is shown that grisms, a grating and prism combination, are a simple way to achieve chromatic control in 3D multi-plane imaging. A pair of grisms, whose separation can be varied, provide a collimated beam with a tuneable chromatic shear from a collimated polychromatic input. This simple control permits the correction of chromatic smearing in 3D imaging using off-axis Fresnel zone plates and improved control of the axial profile of a focussed spot in multi-photon experiments.

OCIS codes: (050.1970) Diffractive optics; (110.4190) Multiple Imaging; (110.6880) 3D Image Acquisition; (170.0180) Microscopy; (180.6900) 3D Microscopy.

References and links

1. D. Toomre and J. Bewersdorf, "A new wave of cellular imaging," Annu. Rev. Cell Dev. Biol. **26**(1), 285–314 (2010).
2. P. A. Dalgarno, H. I. C. Dalgarno, A. Putoud, R. Lambert, L. Paterson, D. C. Logan, D. P. Towers, R. J. Warburton, and A. H. Greenaway, "Multiplane imaging and three dimensional nanoscale particle tracking in biological microscopy," Opt. Express **18**(2), 877–884 (2010).
3. H. I. C. Dalgarno, P. A. Dalgarno, A. C. Dada, C. E. Towers, G. J. Gibson, R. M. Parton, I. Davis, R. J. Warburton, and A. H. Greenaway, "Nanometric depth resolution from multi-focal images in microscopy," J. R. Soc. Interface **8**(60), 942–951 (2011).
4. P. M. Blanchard and A. H. Greenaway, "Broadband simultaneous multiplane imaging," Opt. Commun. **183**(1-4), 29–36 (2000).
5. F. He, H. Xu, Y. Cheng, J. Ni, H. Xiong, Z. Xu, K. Sugioka, and K. Midorikawa, "Fabrication of microfluidic channels with a circular cross section using spatiotemporally focused femtosecond laser pulses," Opt. Lett. **35**(7), 1106–1108 (2010).
6. W. A. Traub, "Constant-dispersion grism spectrometer for channelled spectra," J. Opt. Soc. Am. A **7**(9), 1779–1791 (1990).
7. T. H. Dou, R. Tautz, X. Gu, G. Marcus, T. Feurer, F. Krausz, and L. Veisz, "Dispersion control with reflection grisms of an ultra-broadband spectrum approaching a full octave," Opt. Express **18**(26), 27900–27909 (2010).
8. E. A. Gibson, D. M. Gaudiosi, H. C. Kapteyn, R. Jimenez, S. Kane, R. Huff, C. Durfee, and J. Squier, "Efficient reflection grisms for pulse compression and dispersion compensation of femtosecond pulses," Opt. Lett. **31**(22), 3363–3365 (2006).
9. S. Kane and J. Squier, "Grism-pair stretcher-compressor system for simultaneous second- and third-order dispersion compensation in chirped-pulse amplification," J. Opt. Soc. Am. B **14**(3), 661–665 (1997).
10. K. Glazebrook, "LDSS++ commissioning report," AAO Newsletter **87**, 11–15 (1998).
11. G. J. Hill, M. J. Wolf, J. R. Tufts, and E. C. Smith, "Volume Phase Holographic (VPH) Grisms for Optical and Infrared Spectrographs," Proc. SPIE **4842**, 1–9 (2003).
12. K. Nakajima, N. Ebizuka, M. Iye, and K. Kodate, "Optimal Fabrication of Volume Phase Holographic Grism with High Efficiency and High dispersion, and its application for astronomical observation," Proc. SPIE **7014**, 70141Q (2008).
13. N. Ebizuka, K. S. Kawabata, K. Oka, A. Yamada, M. Kashiwagi, K. Kodate, T. Hattori, N. Kashikawa, and M. Iye, "Grisms developed for FOCAS," Publ. Astron. Soc. Jpn. **63**, S613–S622 (2011).
14. C. Palmer and E. Loewin, *Diffraction Grating Handbook*, 6th ed. (Newport Corp., 2005).

#171880 - $15.00 USD Received 3 Jul 2012; revised 15 Aug 2012; accepted 19 Aug 2012; published 24 Aug 2012

15. P. M. Blanchard and A. H. Greenaway, "Simultaneous multiplane imaging with a distorted diffraction grating," Appl. Opt. **38**(32), 6692–6699 (1999).
16. S. Djidel, J. K. Gansel, H. I. Campbell, and A. H. Greenaway, "High-speed, 3-dimensional, telecentric imaging," Opt. Express **14**(18), 8269–8277 (2006).
17. Private communication from S Abrahamsson

1. Introduction

Microscope imaging techniques can now routinely deliver sub diffraction limited real-time imaging [1]. There is an increasing need to extend these techniques into the third dimension, ideally with a multi-spectral capability, so that dynamic interactions between two or more components can be studied in whole living cells. We have recently demonstrated a simple, on axis multi-plane imaging technology that delivers real time 3D imaging over cellular volumes [2, 3]. Our technique utilizes a diffractive optical element (DOE), in the form of an off axis-Fresnel zone plate, to image multiple object planes simultaneously on a single image plane. Our DOE based 3D imaging has been used in all wide-field imaging modes, e.g. bright-field, fluorescence, phase-contrast etc. It is compatible both with particle localization and tracking and with full-field, 3D, deconvolution-based specimen reconstructions from z-stacks. Z-plane separations of multi-focal images obtained using the DOE-based system can be varied from arbitrarily small to many microns [2, 3]. For full-field imaging, Nyquist z-plane separations allows for volumetric data to be gathered up to 9 times faster, through the simultaneous acquisition of multiple, in-focus specimen planes. Alternatively, by utilizing the defocussed information contained within multiple specimen planes, single particles can be tracked and localized to sub 10 nm axial accuracies through full cell (10 μm) volumes using 9-planes and modest plane separations, e.g. 1 μm [3]. However, due to the need to limit chromatic distortion, the DOE-based technique is narrow band, limiting the incident spectral bandwidth, restricting photon flux and hindering application to multiple-fluorophore life science imaging. Control of this chromatically-induced lateral smearing has been demonstrated by creating a collimated beam in which the spectral components are laterally displaced [4]. This method used a pair of reflective gratings and a folded optical path to compensate for the chromatic distortion by introducing an opposing chromatic shear, a technique also used for controlling the 3D intensity profile in multi-photon processes [5]. Unfortunately, this approach is limiting. The amount of chromatic shear is controlled by changing the distance between the gratings but, because of the folded path, changing the grating separation necessitates adjustments of the angle and/or position of various optical components. Adjusting these additional parameters complicates the control system, making it harder to integrate into user instrumentation and restricting practical application.

We demonstrate the use of a pair of grisms (a grating combined with a prism) in multi-plane polychromatic imaging using a Fresnel zone plate, exploiting the inherent chirp of the DOE to achieve a near-complete correction of the principal chromatic defects in the 3D imaging by simply changing the grism separation in an unfolded, axial, optical system.

Grisms of the sort discussed here were introduced by Traub [6] as a simple way to realize a (nearly) constant-dispersion spectrometer using a single grism to balance the opposite-sense non-linearities of prism and grating dispersion. Grisms have subsequently been widely used in astronomy and in femtosecond laser systems for pulse stretching/compression [7–13]. Both reflective and transmissive grisms have been used, but not the use of a transmissive grism in which a selected wavelength can be un-deviated – a possibility in the original suggestions by Traub and illustrated in the Diffraction Gratings Handbook [14]. It is this configuration, in which first-order diffraction of a selected wavelength occurs for an un-deviated beam, that is exploited here to provide a simplified chromatic control system.

In the following we describe the fabrication of the grism pair using commercially-available prisms and transmissive blazed gratings, as described in [6]. Our grisms are designed to give an un-deviated wavelength in the mid visible where many biologically-

#171880 - $15.00 USD Received 3 Jul 2012; revised 15 Aug 2012; accepted 19 Aug 2012; published 24 Aug 2012

useful fluorophores emit. This grism pair is used in tests to achieve a collimated output beam with easily-varied chromatic shear. We assess the chromatic shear produced as a function of the grism separation by measuring the angle at which two different laser wavelengths are brought to focus as a function of the grism separation. We then demonstrate correction of dispersion in 3D imaging of a compact polychromatic source using off-axis Fresnel zone plates. The measured performance of our grisms, assembled from easily-available commercial off the shelf (COTS) components, will be compared with a ray-tracing model in order better to assess the performance expected from grisms designed for this application.

2. Grism fabrication

Ideally our grism should consist of a prism and a blazed transmission grating made from the same material (thus same refractive index) with the grating blaze angle equal to the wedge angle of the prism. The grating is then cemented to one side of the prism so that the exterior faces of the grating facets are parallel to the input face of the prism, Fig. 1. However, for these proof of principle experiments we have assembled our grisms from COTS components. An optical ray-tracing simulation (Zemax) was performed to select a suitable combination of components. The model showed that an N-BK7 prism with a wedge angle of 21°30′ combined with a 300 grooves per mm transmission grating would provide appropriate dispersion. From COTS components available we selected an 18°8′ wedge-angle prism fabricated from N-BK7 and a B270 transmission grating of 300 grooves/mm and a blaze angle of 17°30′ (from Edmund Optics), giving a 'straight-through' wavelength of 538.5nm. The prisms and gratings were cemented together to make the grisms in an optical workshop.

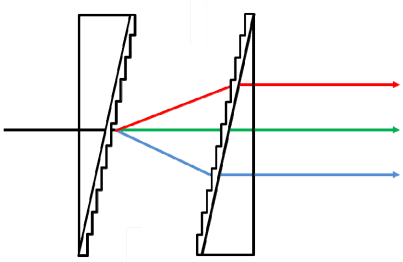

Fig. 1. Schematic of a pair of identical, back to back grisms used to produce a collimated beam with chromatic shear from a collimated polychrome input. The lateral shear between the polychrome components in the output beam is controlled by varying the separation between the grisms.

These grisms were mounted back to back in custom mounts within an assembly using opto-mechanical components (Thorlabs). Our custom mounts allow the input faces of the grisms to be rotated in the horizontal with respect to the optical axis with accuracy of ~2 degrees. The blazed surfaces of the grisms are quite fragile and represent a significant disadvantage of this design. The opto-mechanics allows for the grism separation to be varied, to within an accuracy of approximately ± 1mm, over a range from 3 to 154 mm, the lower figure selected to protect the fragile gratings. Figure 1 shows a schematic of the grism configuration in our experiments.

3. Experimental tests

Chromatic image tests

A simple test was conducted to assess chromatic shear produced by the grism-pair, as shown schematically in Fig. 2. Two lasers, of wavelengths 543 nm and 633 nm, were coupled through a beamsplitter and ND (neutral density) filters, not shown in Fig. 2, and fed through an optical fibre (Thorlabs SM600 fiber, single mode at 633 nm) to provide a compact

#171880 - $15.00 USD Received 3 Jul 2012; revised 15 Aug 2012; accepted 19 Aug 2012; published 24 Aug 2012

polychromatic source. The light from this fibre was collimated by an achromat (focal length 30 mm) to provide an approximately 3 mm diameter beam. The collimated beam was refocused by a second achromat (focal length 250 mm) chosen to give well-sampled images with the 6.45 μm CCD pixels (Qimaging Retiga). The separation between the lenses was 300 mm and the maximum separation between the inner faces of the grisms 154 mm. Figure 2 shows black broken lines to illustrate ray paths and position of focus if no grisms are used, and black solid/coloured lines for use with grisms.

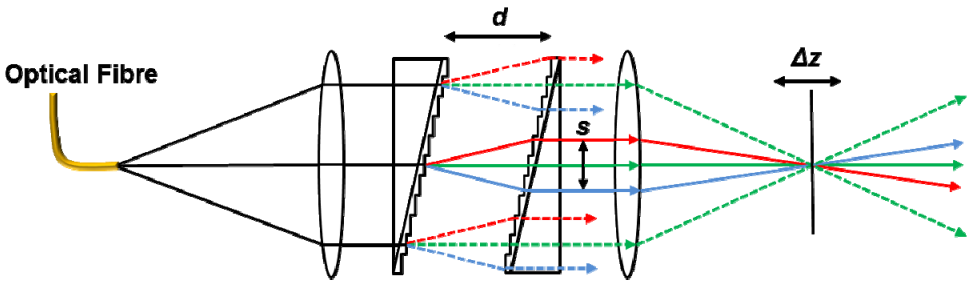

Fig. 2. Schematic of the 1st experiment. Black arrows indicate how the chromatic shear, *s*, is changed by varying grism spacing, *d*. After the grism only the on-axis rays (solid) are shown in full, the off axis paraxial rays (dashed) are truncated for clarity. The angle at which the laser beams come to focus is assessed by scanning the camera axially about the 'best focus', as indicated *Δz*.

Images with both lasers incident were recorded as a function of camera position as the camera is translated ± 10 mm either side from the 'best focus' image plane for variety of grism separations, Fig. 3. The NDs were adjusted so that both laser lines were matched in intensity and, in combination, did not saturate the camera. Figure 3(a) shows that, through the 'best focus' image plane, there is a clear shift of the 633 nm spot relative to the 543 nm spot. The 543 nm spot remains largely fixed as it is close to the un-deviated wavelength of the grism pair. Figure 3(a) demonstrates the potential for chromatic tuning using an on-axis grism pair. By repeating the measurements as a function of grism distance, Fig. 3(b), the angle of arrival of chromatic components can be estimated and, using the focal length of the imaging lens, the spatial chromatic shear produced by the grism separation (0.0294 mm shear between the laser beams per mm separation, equivalent to 327 μm shear per nm bandpass per mm of grism separation) can be deduced, Fig. 3(c).

#171880 - $15.00 USD Received 3 Jul 2012; revised 15 Aug 2012; accepted 19 Aug 2012; published 24 Aug 2012

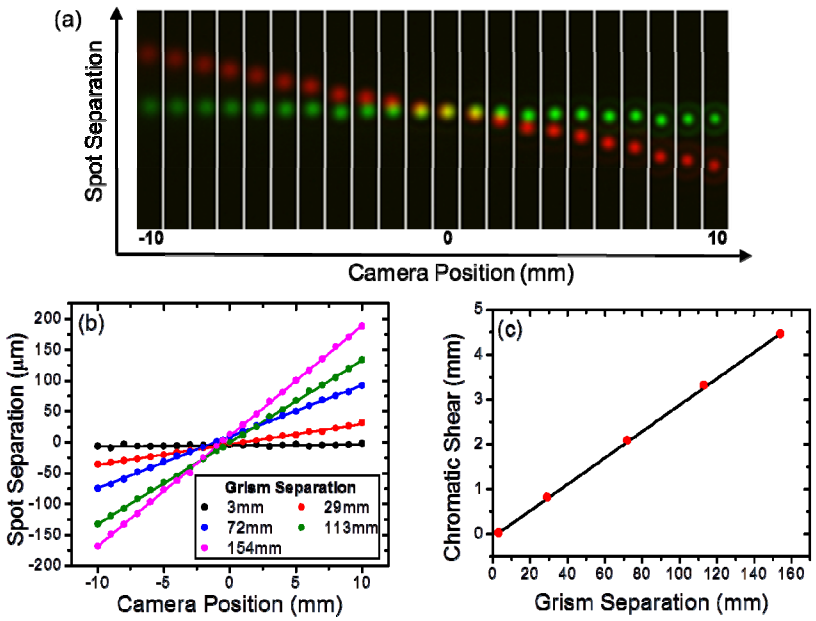

Fig. 3. a) False-colour montage showing the separation of the image of the fibre source in each laser line as a function of camera distance from 'best focus'. b) Shows the image separation as a function of camera position for various grism separations, using data of which (a) is an illustration for grism spacing 154 mm. c) The spatial chromatic shear produced by varying grism separation and deduced from (b) using the lens focal length.

Combining the chromatic angle of arrival control achieved using the grisms with accurate chromatically-dependent timing of the spectral components in a femtosecond laser pulse (not demonstrated in these experiments) provides a simple control system by means of which the 3D profile in multi-photon laser inscription [5] can be dynamically tuned. In laser-inscription applications where control of the axial focus quality is desired, a high NA objective would be used. Here, of course, only the spatio-chromatic properties of the focus can be assessed.

3D imaging tests

3D imaging using an off-axis Fresnel zone plate DOE (a phase grating with quadratic distortion) is based on the simultaneous focus of multiple object planes on a single image plane using a simple, on axis optical set-up [15]. The DOE imparts a different focusing power in each diffraction order, with a linear dependence of focal length on incident wavelength [4]. We have previously demonstrated the effectiveness of this approach to 3D imaging in biological systems and applied to super resolution 4D particle localization [2, 3]. However, the DOE introduces a natural chromatic smearing in the non-zero orders [4]. In our previous work narrow-band filters, ~10 nm, have been used to reduce this effect to a few camera pixels. Unfortunately, this still induces some chromatic smearing and significantly reduces available photon flux, thus restricting practical biological applications. However, by definition the DOE period is linearly chirped along one axis, and that chirp can be used to our advantage. By pre-dispersing the polychrome input beam using the grism pair, each incident wavelength is positioned within the chirped zone plate to 'see' the same DOE structure measured in wavelength units. The pre-dispersion thus equalises the angle of diffraction for each wavelength, giving non smeared, 'white light' images in all diffraction orders.

To test the grism correction in DOE-based 3D imaging we mounted the grism pair between two 400 mm achromatic lenses, as shown in Fig. 4(a). The lenses, spaced 200 mm apart, operate as a unit magnification relay system with an effective focal length of 266 mm.

#171880 - $15.00 USD Received 3 Jul 2012; revised 15 Aug 2012; accepted 19 Aug 2012; published 24 Aug 2012

When the DOE is placed 266 mm from the second principal plane (133mm from the second lens) of the compound imaging system equal magnification images are obtained in each diffraction order, providing simultaneous multi-plane imaging due to the order dependent focusing power introduced by the DOE [4, 15, 16]. Note that only the spacing between the two grisms is relevant, not their absolute position between the achromat pair.

This imaging system was tested with the dual laser system previously described and with a multimode white light source (quartz halogen) filtered using a set of 20 nm bandpass filters with central wavelengths from 450 nm to 690 nm. Because a single polychromatic source was used in these experiments it was necessary to scan the source position to record the 3D foci in the different diffraction orders. These images were recorded with and without using the grism system. When the grisms were introduced, c.f. Figure 4(a), the grism spacing *d* was chosen as accurately as possible to equalize the diffraction angles at all wavelengths.

Figure 4(b) demonstrates, for the −1 diffraction order, the principle of the chromatic correction. Figure 4(bi) show the results of the single mode launched dual laser illumination used in Fig. 3. At grism spacing of 68.6 mm the chromatic smearing over the 90 nm bandpass is neutralized. The diffractive optical element (DOE) used has a nominal axial period of 45 μm, a curvature, W_{20} of 150 waves and radius 11mm and therefore a focal length 733 mm at 550 nm wavelength [4, 15]. A chromatic shear of 15.2 μm per nm of bandpass is required across the chirped DOE in order to equalize the angle of dispersion across the optical bandpass. For the 90 nm bandpass between the lasers used, the total chromatic shear required between the two beams is thus 1.37 mm. This is the shear required at the DOE, allowing for the beam convergence to the camera, this corresponds to 2.05 mm of shear before the final lens. For Fig. 3(c), a grism spacing of 68.6mm corresponds to a shear of 1.96mm.

Figure 4(bii-iv) shows images of a 50 μm core fibre-launched white light filtered by a range of 20 nm bandpass filters (Thorlabs) with central wavelengths from 450 nm to 690 nm in 20 nm steps, and with each image normalized for equal total photon flux at each bandpass. (ii) shows the falsely coloured image obtained by focusing the system for 550 nm central wavelength with and without grism correction (and without adjusting for the linearly wavelength dependent focusing power of the zone plate, this second-order effect accounts for the 'bow tie' structure in the data). Chromatic smearing is effectively removed by the grisms, leaving a single un-smeared spot. The image quality is dominated by a residual λ dependence of the focal length of the DOE [4]. To demonstrate the true range of the chromatic correction (iii) repeats the same experiment as (ii), but with the source repositioned at each bandwidth to compensate for the DOE-induced focal dependence. Images in the + 1 order (not shown) show identical results. Chromatic smearing is effectively removed by the grisms across the green and red wavebands, but not as effectively in the blue band. Comparison of top and bottom images in Fig. 4(biii) shows that the chromatic smearing has been reduced by a factor of 6.5. Residual chromatic smearing may be due to deviations from linearity in the grism dispersion and/or minor imprecision in component positioning. Finally (iv) shows that, in the DOE's 0th order image, which inherently has no chromatic distortion as it is unaffected by the DOE, the grisms have no effect on the image. Figure 4 demonstrates the successful use of the grism pair for correction of the chromatic dispersion of the Fresnel zone plate.

The combination of wavelength, DOE axial period and DOE to camera distance determines the lateral separation of the in-focus specimen-slice images on the camera. The focal length of the Fresnel lens combined with the focal length of the imaging lens determines the axial separation of the in focus planes [16] which, for the combination focal length and the Fresnel lens used here produces, for λ = 550 nm, a separation of 97 mm between the in-focus specimen planes. In microscopy applications, this separation is related back to the specimen through a scaling dependent on the image magnification squared [2, 3].

#171880 - $15.00 USD Received 3 Jul 2012; revised 15 Aug 2012; accepted 19 Aug 2012; published 24 Aug 2012

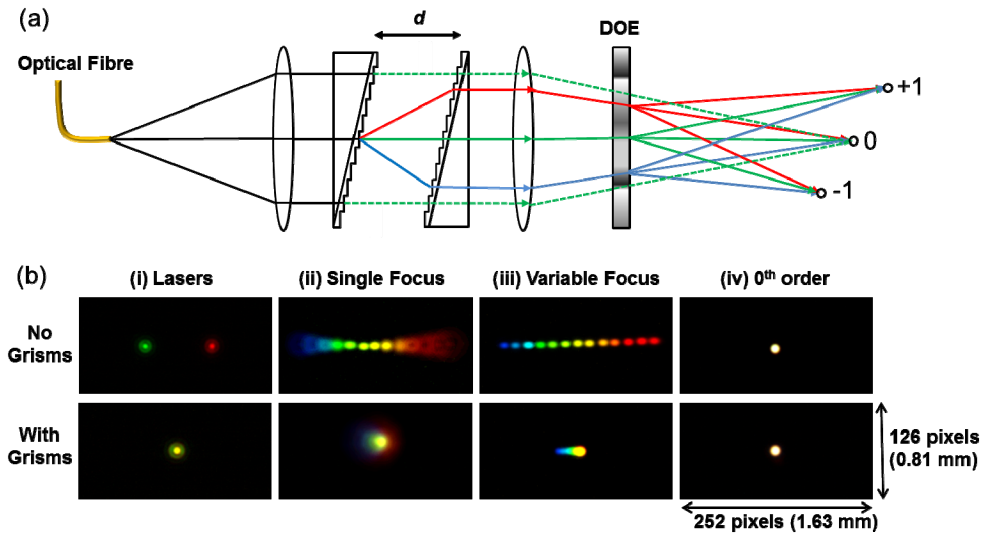

Fig. 4. (a) Schematic of the grism system used to correct chromatic blur in a 3D imaging system using a DOE in the form of an off-axis zone plate. The 3 foci shown on the right illustrate the position of focus of the single fibre source in each diffraction order and when the single source position is fixed. On a single, flat camera plane each diffraction order is focussed on a different specimen plane and the 3 foci are recorded simultaneously. In our measurements the zone plate has a 733mm focal length in the −1 diffraction order at 550nm and has a nominal axial period 45 μm; (b) False colour images from a (i) dual laser input and (ii-iv) bandpass-filtered white light source, in each case the total integrated images intensity has been equalised in each colour band. (i) 633 nm and 543 nm laser with and without grism correction. (ii) filtered white light input at a single focus (iii) filtered white light input at optimal focii for each colour and (iv) filtered white light input of the 0th order, showing unmodified images with and without grisms.

Because of the chirp, deliberate lateral translation of the DOE can be used to change the separation of the in-focus image slices on the camera without changing their z-separations within the specimen field. This provides a valuable mechanism to adjust for different cameras and to modify the field of view to optimize for any given camera. However, such lateral displacement of the DOE from its nominal axial position also changes the amount of pre-dispersion required to achieve chromatic correction of the multiple, in-focus images that the DOE-based 3D imaging system provides. Our grism pair provides the flexibility to adjust the chromatic shear to compensate for any such re-alignment required to optimize the system for different cameras.

4. Application for multi-colour fluorescence microscopy

The results shown in Fig. 3 and 4 assess the performance of the grism correction in 'white light' measurements over the entire visible spectrum. However, one of the principal applications for the DOE-based 3D imaging is in fluorescence microscopy, allowing access to the full bandwidth of the fluorophore used for 3D imaging. We simulate the performance of the grism correction to fluorophore imaging by modifying the bandpass filtered white light approach outlined in section 3 and simply summing a series of images spanning the fluorophore bandwidth, with an appropriate weighting to mimic the fluorophore spectrum (Fig. 5). Importantly, as will be shown, the limiting bandwidth of most fluorophores, < 100 nm, and the fluorophore spectral profile, combined with the grism correction, effectively remove the image blurring due to the λ dependence of the focal length of the DOE.

As an illustration we have chosen to model eGFP, Cy5 and mCherry, three fluorophores widely used in cell biology. For each fluorophore the system was focused and aligned for the

#171880 - $15.00 USD Received 3 Jul 2012; revised 15 Aug 2012; accepted 19 Aug 2012; published 24 Aug 2012

filter that best matched the peak fluorophore wavelength (520, 570 and 610 nm respectively). With the source position fixed for each fluorophore, a series of narrow band images were then recorded using a set of spectral filters covering the fluorophore emission spectrum. The spots corresponding to the individual filters are clearly visible. To process the images, the total flux for each filter is first normalized to the total flux at the peak wavelength and then weighted to simulate the fluorophore spectrum by the appropriate factor, Fig. 5(a)-5(c). The composite 'fluorophore' images for each simulated fluorophore, with and without grism in place, are shown in Fig. 5(d). Once again chromatic smearing is effectively removed.

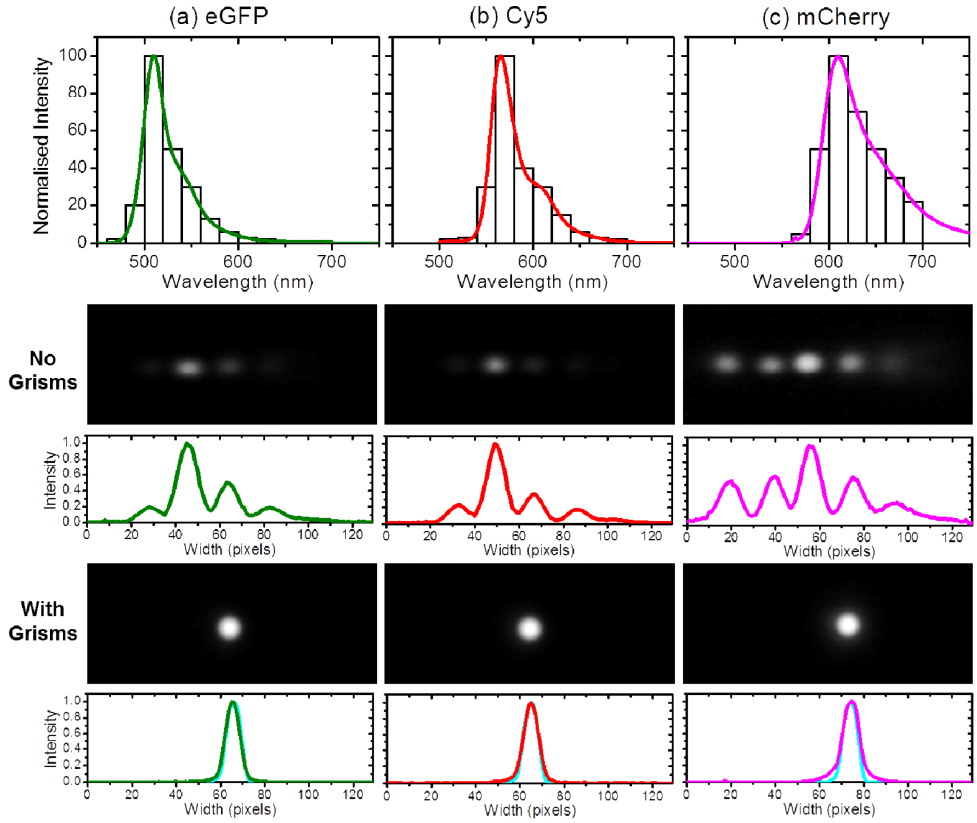

Fig. 5. Simulation of chromatic correction applied to fluorophore imaging. (a)-(c) normalised spectrum for eGFP, Cy5 and mCherry with overlayed, weigthed, 20 nm bandpass slices used to model spectral form using white light. (d) Monochrome images of the fluorophore image, simulated from bandpass weighting as in (a)-(c) with and without grism correction. The panels in (d) show show images and sectional profile through the imaged spots. The sectional profile 'with grisms' also shows an ideal profile of a narrow band spot (cyan, 3nm bandpass) that represents ideal imaging of the 50 µm fibre source.

We quantify the performance of the grism correction by comparing the horizontal cross section through the composite images (lower panels Fig. 5(d)) with that of a single image taken with narrow band (3 nm, 633 nm) illumination through the same 50 µm fibre, shown in the same panels in cyan. For eGFP and Cy5 the spot sections accurately match that for the narrow-band 633 nm filter. For the broader bandwidth mCherry, there is evidence of some residual chromatic smearing manifest in some low-brightness 'wings'.

The simultaneous use of multiple fluorophores to facilitate studies of the interactions between cellular components is important in many biological studies and the results obtained permit us to assess the use of the system described for 3D, multi-colour, multiple-focus microscopy. Using a dual DOE system (each etched for a different wavelength), a single

#171880 - $15.00 USD Received 3 Jul 2012; revised 15 Aug 2012; accepted 19 Aug 2012; published 24 Aug 2012

grism pair and a dichroic mirror between the DOE and camera, allows one to form multi-focus images simultaneously on two separate monochrome cameras. If the dichroic directs emission from a short wavelength emission fluorophore to one camera and the other camera sees a long wavelength fluorophore, these fluorophores can both be imaged separately but simultaneously in 3D on the two cameras. A third fluorophore at a central wavelength can be chosen such that the light from this fluorophore is detected in 3D on both cameras. The coincident images on the two cameras are clearly due to the mid-wavelength fluorophore and, once these coincidences have been established, the remaining images on each camera can be assigned to the appropriate long or short wavelength fluorophore. Since each fluorophore is thus imaged simultaneously in 3D, it is possible to study dynamic interactions between three different cellular components in 3D with accurate chromatic correction.

5. Discussion / conclusion

The two sets of tests presented here, using a simple grism pair fabricated from COTS components, demonstrate the ease with which grisms of this design can be incorporated into complex optical systems in order to achieve a variable chromatic shear on an input beam without changing the convergence properties of the beam. This claim is verified by considering, for the 3D imaging system, that the position of the in-focus images in different colour, shown in Fig. 4(biii), is entirely consistent with the expected shift in focus evaluated from the chromatic variation of the zone-plate focal length.

The chromatic focus control used to evaluate the chromatic shear as a function of grism separation can also be used to achieve control of the 3D field distribution at focus and thus can be used for spatio-temporal control in laser inscription [5]. The chromatic corrections achieved here can be effected with blazed gratings that deviate the beams [4], but such systems are difficult and expensive to maintain in alignment, whereas the system described uses a simple sliding mechanism and thus provides a significantly more practical solution.

One of the prime reasons for developing this system was to implement a simple chromatic correction that would allow us to make effective use of the full fluorophore bandwidth and, for that reason, the optical efficiency of the grism system is of significant interest. For application in 3D live-cell microscopy of fluorescently-tagged live cells [2], where the sources are intrinsically faint and the photon flux may be limited by the inherent photophysics (bleaching, blinking and cyto-toxicity), achieving the highest total optical throughput is very important. High optical efficiency is further crucial in our application, where the need to re-collimate the dispersed beam dictates the use of two identical grisms. With the experimental arrangements that we have used it was not feasible experimentally to assess the optical efficiency, but ray-tracing estimates indicate that an efficiency of 75% is achievable with the grisms used here. However, in the context of the suggested application to 3D imaging the grism pair provides substantial overall flux gains. Without chromatic correction 3D imaging is restricted to, typically, a 10 nm collection bandpass. For mCherry, as an example, at peak $\lambda = 610$ nm a 10 nm bandpass collects only 12% of the overall flux, even at 90% transmission. With grism correction the full fluorophore range can be accessed, giving a 6-fold increase in collected flux levels.

We have successfully demonstrated the ease with which standard, commercial optics can be used in an on-axis grism system. Our optical system is robust and simple to align. Component placement accurate to ± 1 mm axially and ± 1 degree for angular rotation is adequate, and the results presented here rely on manual component placement without the use of precision translation or rotation stages, despite the absence of rotational symmetry in the grisms and the DOE. It is worth considering the advantages of customized, and therefore more expensive, solutions based on Volume Phase Hologram (VPH) grisms [10], in which a holographic grating is sandwiched between a pair of symmetric prisms [11]. Such VPH grisms are expensive but extremely robust, and optical efficiencies of 91.5% have been claimed [12] at 2.2 μm wavelength. Although VPH grisms appear to offer higher optical

#171880 - $15.00 USD Received 3 Jul 2012; revised 15 Aug 2012; accepted 19 Aug 2012; published 24 Aug 2012

efficiency [13], they represent a significantly increased cost and complexity over the cheaper surface-relief grisms described by Traub.

Future modifications can easily optimize performance and operation. In a custom system the grism pair can be optimized for ideal on axis throughout at a chosen wavelength, typically the central of the input bandwidth. In practical terms the angular controls required within the grism system are independent of grism separation and can be locked when the system is constructed. The grism separations can be easily controlled by a simple motor-driven translation in future systems. The grism orientation used in all of these experiments and designs was such that the prism faces were outermost in the grism pair. Reversing this arrangement so that the blazed grating are outermost offers further control possibilities, in that the interior prism faces in such an arrangement provide some additional chromatic control through the refraction of all but the un-deviated wavelength. A ray-tracing study shows that this arrangement offers slightly better linearity in the dispersion. A further possibility is the use of two grisms of slightly-different design, rather than a pair of (nominally) identical grisms back to back as described here. Such an arrangement would permit the images on the camera to be separated chromatically, for example if different colour fluorophores are required. A different implementation of similar principles has been investigated elsewhere [17].

In conclusion we have demonstrated the use of a simple, linear, grism (grating and prism) pair to remove chromatic smearing in DOE based 3D imaging application without compromising image quality. Beyond 3D imaging this simple system has application in two-photon laser inscription.

Acknowledgment

This work at Heriot-Watt University was funded by the Science and Technology Facilities Council (STFC). YF acknowledges receipt of a Scottish Universities Physics Alliance (SUPA) Prize Studentship and, previously, a China Scholarship Council (CSC). YF also acknowledges the support of her home supervisor, Professor Jiaru Chu of University of Science and Technology of China.

#171880 - $15.00 USD Received 3 Jul 2012; revised 15 Aug 2012; accepted 19 Aug 2012; published 24 Aug 2012